7. E. Iliel, N. Allinzher, S. Enzhial, and G. Morrison, Conformational Analysis [in Russian], Moscow (1969).
8. P. Nagy, Acta Chim. Acad. Sci. Hung., 108, 401-412 (1981).
9. T. Ikeda and R. C. Lord, J. Chem. Phys., 56, No. 9, 4450-4466 (1972).
10. H. E. Howard-Lock and G. W. King, J. Mol. Spectrosc., 35, No. 3, 393-412 (1970).
11. V. B. Kartha, H. H. Mantsch, and R. N. Jones, Can. J. Chem., 51, 1749-1766 (1973).
12. N. Nakamura, H. Suga, and S. Seki, Bull. Chem. Soc. Jpn., 53, No. 10, 2755-2761 (1980).
13. G. Wolf, Helv. Chim. Acta, 55, Fasc. 5, No. 143, 1446-1459 (1972).
14. P. Sellers and S. Sunner, Acta Chem. Scand., 16, No. 1, 46-52 (1962).

# PARAMETRIC STUDY OF SPARK BREAKDOWN ACCOMPANYING SUCCESSIVE IGNITION OF DISCHARGE GAPS IN PHOTOPREIONIZATION SCHEMES

N. A. Belous, V. A. Vasetskii, and V. N. Karnyushin

UDC 537.523.4

The breakdown and dynamic characteristics of a sectioned spark discharge with successive gap ignition, employed for volume UV preionization, were studied experimentally.

A sectioned spark discharge with successive gap ignition is a simple and effective method of UV preionization for producing volume-uniform discharges at high pressures. Sequential sectioning makes it possible to realize an aperiodic discharge with a steep front and short duration, which provides high uniformity and high intensity of ionization of the medium [1, 2]. The determining factors of the ionizing efficiency of spark discharges are the current strength and the rate of change of the current [3, 4]. In this connection, together with the breakdown and energy characteristics, processes occurring at the formation stage of the discharge and the development dynamics of the discharge are of considerable practical interest.

The purpose of this work is to carry out a parametric investigation of the breakdown and energy characteristics, as well as the dynamics of formation and development of a multispark discharge with sequential sectioning for a wide range of geometric and circuit parameters.

The scheme used to form the discharge is shown in Fig. 1a. Linear chains of spark gaps with a distance of 1 mm between the electrodes and electrodes 0.8 mm in diameter were employed. The scale of sectioning is determined by the sizes of the intermediate capacitors. In the experiments performed the distance between the spark gaps equaled 10 mm, and the distance between the gaps and the reverse current conductor equaled 25 mm. The discharge was created in air at atmospheric pressure. Power was fed to the discharge by means of negative voltage pulses with an approximate 20 nsec leading edge and a characteristic exponential decay time of 4 μsec.

The measurement procedure included oscillographic recording of the current and voltage as well as the scan of the discharge emission with an image convertor tube. The voltage on the charging capacitor and at different points along the discharge chain was determined with the help of ohmic dividers. The discharge current was measured with the help of low-inductance shunts at the beginning and end of the discharge line ($I_1$ and $I_2$ in Fig. 1a). The intermediate capacitance, the number of gaps, and the amplitude of the voltage pulse were variable parameters.

It was established experimentally that the process of formation of a multispark breakdown with successive sectioning occurs in three stages. This is illustrated by the typical oscillograms of the current and voltage and scanning of the discharge emission (see Figs. 1b and c). At the first stage, whose duration is $\tau_1 = t_1 - t_0$, sequential breakdown of the gaps, maintained by the charging of the intermediate capacitors $C_i$, occurs. This stage is

A. V. Lykov Institute of Heat and Mass Transfer, Academy of Sciences of the Belorussian SSR, Minsk. Translated from Inzhenerno-Fizicheskii Zhurnal, Vol. 52, No. 5, pp. 812-817, May, 1987. Original article submitted March 24, 1986.

0022-0841/87/5205-0595$12.50  

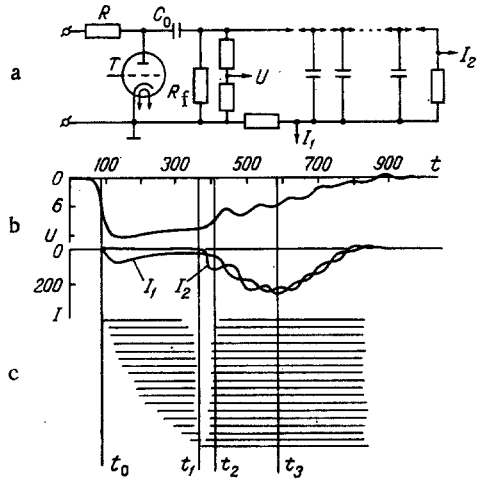


Fig. 1. Diagram of the electrical circuit (a), oscillograms of the voltage and current (b), and scan of the emission (c) from the discharge: $R_k$) discharge resistance, $R_f$) forming resistance; T) a TGI 1-1000/25 thyrotron, $C_0$) a 10-nF charging capacitor; $C_i$) intermediate capacitors. U, kV; I, A; t, nsec.

characterized by a weak discharge current $I \approx \partial(C_i U)/\partial t$ and a small voltage drop. Thus, for example, for threshold breakdown voltages and $C_i \approx$ 20 pF the amplitude of the current changes from 30 to 70 A as the number of gaps increases from 10 to 50.

Figure 2 shows the voltage distribution on the spark gap along the discharge line for the characteristic times marked in Figs. 1b and c. At the end of the first stage a voltage distribution (curve $t_1$) characterized by a small voltage drop on the total discharge gap and a sharp drop at the end is formed. The determining factor in the further growth of spark channels at the second stage with a duration $\tau_2 = t_2 - t_1$ is the process of discharge of the intermediate capacitors. This damped oscillatory process in the circuit of the discharge line continues throughout the entire lifetime of the discharge, and in addition the period of the oscillations equals 50-100 nsec for 10-50 gaps, while the amplitude decreases approximately by a factor of two over one period. This is illustrated by the oscillograms of the current $I_2$ and voltage of the discharge (see Fig. 1b). Together with this, during the second stage current continues to flow from the generator through the total discharge gap. As a result, by the time $t_2$ a monotonically decreasing voltage distribution is established along the discharge line (Fig. 2) and the main discharge current pulse is formed. The second stage is also characterized by a weak current $I_1$ and a sharp rise in the current $I_2$. For example, for N = 50 and U = 14 kV the amplitude $I_2$ = 350 A.

The experiments described showed that the velocity of propagation of the breakdown at the first stage changes substantially along the discharge line. It is obvious from a scan of the discharge emission (Fig. 1c) that at the end of the discharge line the velocity decreases. This is attributable to the decrease in the amplitude of the voltage wave as the discharge propagates along the line, since the resistance of the total discharge gap increases. At the second stage the breakdown grows rapidly, virtually independently of the overvoltage when the number of gaps is large enough. As the amplitude of the voltage pulses increases the durations of the first two stages gradually converge toward one another. The strengths of the currents $I_1$ and $I_2$ increase monotonically at the same time. The duration of the main (third) stage of the discharge for a fixed number of gaps remains virtually unchanged as the voltage increases, since it depends primarily on the inductance of the discharge circuit.

Figure 3a shows the dependence of the threshold breakdown voltage on the magnitude of the intermediate capacitance $C_i$. The magnitude of the intermediate capacitance varied from 2.7 to 94 pF. One can see that in the range $C_i \geqslant 20$ pF the breakdown voltage is virtually independent of the intermediate capacitance, which makes it possible to select an optimal

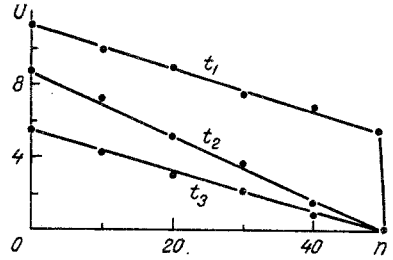


Fig. 2. Distribution of the voltage along the discharge line at different times; n is the number of the discharge gap. N = 50, $t_1$, $t_2$, and $t_3$ are defined in Fig. 1.

value of the intermediate capacitance from the condition that the working voltages be minimum. This nature of the dependence of the breakdown voltage shows that in order to ignite a sequential spark discharge a definite energy input $E \approx 0.5C_iU^2$ in each gap is required. Up to values $C_i \approx 20$ pF this magnitude is constant and then increases in proportion to the increase in $C_i$.

As one can see from Fig. 3b, the dependence of the breakdown voltage on the number of gaps in the range N = 10-50 is virtually linear. Losses at the formation stage of the discharge strongly affect the magnitude of the breakdown voltage and the slope of the linear section of the dependence. Curve 1 was obtained with a multirow configuration of the discharge lines with a dense assembly of the intermediate capacitors and using a pulse generator with a forming resistance. Under these conditions the drop in the amplitude of the voltage pulse up to the beginning of the main stage of the discharge, owing to energy losses in the forming resistance and the presence of the circuit capacitor between neighboring gaps, equalled about 15%. With a uniform configuration of the discharge line the circuit capacitance decreases by a factor of two, and as a result the breakdown voltage drops approximately by 30% (curve 2). With the use of an inductance as the forming element in the pulse generator there is virtually no voltage drop at the formation stage, which leads to an additional reduction of the breakdown voltage (curve 3). Thus losses at the formation stage of the discharge can double the working voltages.

In order to clarify the effect of the mutual arrangement of the gaps on the breakdown voltage we studied a zigzap-shaped configuration of the discharge chain with a periodicity of five cells. The experiments showed that compared with the linear configuration the breakdown voltage increased approximately by 2 kV. This can be explained by the fact that for a zigzag-shaped configuration the intermediate capacitors can be percharged as a result of emission of electrons and photoionization of the gas, as well as a result of the circuit capacitance between the cells, constituting $\sim 0.3C_i$ under the conditions of the experiment.

A hydrogen thyrotron is the most useful commutator for the operation of preionization systems in the repetitive pulse mode. The use of hydrogen thyrotrons imposes a restriction on the load resistance and the reverse voltage owing to overcharging of the charging capacitor. For example, for the TGI 1-1000/25 thyrotron the magnitude of the reverse voltage owing to the mismatch should not exceed 5 kV. The ratio between the critical resistance of the discharge circuit and the active resistance, equal to $R/R_{cr} = 0.5$, can be used as the condition limiting the maximum working discharge voltages and satisfying these requirements. In this case the transfer factor for transferring the energy in the charging capacitor into the active component of the load equals 0.95, while the magnitude of the reverse voltage does not exceed 20% of the charging voltage.

Figure 4 shows the dependence of the amplitude of the current pulse on the voltage for a different number of gaps. The lower limit of the family of curves is determined by the breakdown voltages, while the upper limit is determined by the condition $R/R_{cr} = 0.5$, which is realized, beginning approximately with 10 gaps. One can see that the amplitude of the current pulse increases linearly as the voltage increases. As the number of gaps in the discharge line increases the range of values of the current amplitude for the same overvoltage increases. The dependence presented permits choosing optimal values of the discharge

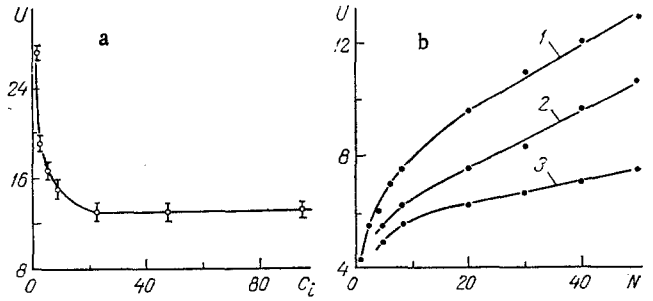


Fig. 3. Breakdown voltage as a function of the intermediate capacitance, N = 50 (a) and as a function of the number of gaps (b): 1) multirow configuration; 2) single-row configuration, $R_f$ = 200 Ω; 3) single-row, forming inductance $L_f$ = 1.1 mH. $C_i$, pF.

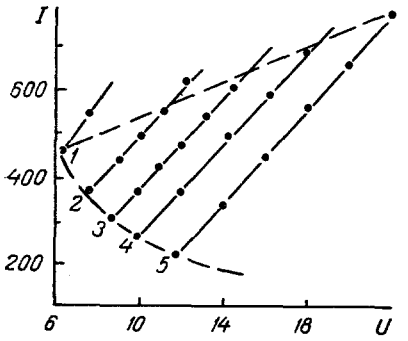


Fig. 4. Dependence of the amplitude of the current pulse on the supply voltage: 1) N = 10; 2) 20; 3) 30; 4) 40; 5) 50.

parameters depending on the conditions of use.

Thus the investigations performed showed that the development of a multispark discharge with sequential sectioning occurs in three stages. At the first stage the sequential breakdown of the gaps is determined by the charging of the intermediate capacitors. The development of the discharge at the second stage is characterized by the oscillatory discharge of distributed intermediate capacitors, as a result of which the voltage required for developing a strong-current discharge is redistributed. At the third (main) stage a self-sustained discharge in preionized gaps is realized. It was shown that in the general case the breakdown and time-dependent characteristics of the discharge are determined by the magnitude of the discharge capacitance, the number of gaps, and the amplitude of the applied voltage pulse. The dependences of the breakdown voltages on the discharge capacitance and the number of gaps were obtained. It was established experimentally that the minimum working voltages are realized with an intermediate capacitance $C_i \approx 20$ pF and increase in proportion to the increase in the number of gaps for N = 10-50. The characteristics of the discharge at the main stage are determined by the magnitude of the applied voltage and by the inductance of the discharge circuit. The oscillatory process in the circuit of the discharge line has virtually no effect on the parameters of the discharge at the main stage. It was established that the formation time of the discharge is determined by the time constant of the discharge line taking into account the distribution of the energy input into the discharge over the stages of the breakdown.

The conditions and scale of the experiments performed make it possible to use the results obtained for the development of practical photopreionization setups.

LITERATURE CITED

1. V. N. Karnyushin, A. N. Malov, and R. I. Soloukhin, Zh. Tekh. Fiz., 48, No. 3, 310-313 (1978).
2. V. N. Karnyushin and R. I. Soloukhin, Macroscopic and Molecular Processes in Gas Lasers [in Russian], Moscow (1981).
3. K. Fol'rat, Physics of Fast Processes [in Russian], Moscow (1971), pp. 96-199.
4. E. P. Velikhov, V. Yu. Baranov, V. S. Letokhov, et al., Pulsed $CO_2$ Lasers and Their Application for Isotope Separation [in Russian], Moscow (1983).

# PRINCIPLES OF DIELECTRIC MATERIAL FAILURE UNDER THE ACTION OF CONCENTRATED ENERGY FLUXES

A. B. Demidovich, G. S. Romanov,
Yu. A. Stankevich, and V. D. Shimanovich

UDC 533.924

The process of failure of silicate material under the action of energy fluxes of $2\cdot10^6$-$1\cdot10^9$ W/m$^2$ is considered. Results of a numerical solution considering fusion, evaporation, and radiation are presented.

Creation of coatings by using lasers and electric arc generators have recently become a practical application, during which thermal fluxes above $1\cdot10^6$ W/m$^2$ are applied to surfaces of parts for lengthy periods under industrial conditions. Motion of the temperature front within a layer of silicate material during action of a flux $q = (1\text{-}2)\cdot10^6$ W/m$^2$ was considered in [1]. It was found that the temperature of the part surface $T_s$ could be significantly higher than the material fusion temperature $T_\zeta$. However the experiments of [2] show that for such fluxes there is little surface fusion for action times of $\sim$1 sec, and consequently, $T_s$ exceeds $T_\zeta$ only insignificantly. The disagreement between calculated and experimental results is apparently the result of [1]'s neglect of fusion and evaporation on the material surface.

In order to determine the possibilities of electric arc processing the present study will investigate heating of silicate materials under the action of thermal fluxes of $2\cdot10^6$-$1\cdot10^9$ W/m$^2$. Calculations will be presented for concrete q values with consideration of the phase transitions referred to above.

The process of coating formation upon a material during thermal processing is characterized by the temperature of the melt surface, the rate of growth of the coating, defined as the difference between the velocities of the fusion and evaporation fronts, and the efficiency, defined by ratio of the energy required for formation of the melt to the amount of energy supplied. Thus, the basic system of equations must describe heat propagation in the solid phase, fusion of the material, evaporation, and cooling of the melt by radiation. In the general case this problem is two-dimensional. However, if the characteristic dimensions of the interaction zone are significantly larger than the region of thermal front propagation in the material, it can be reduced to one-dimensional form. In practice this condition is satisfied both in use of large-size thermal sources and in scanning of limited size sources at a rate higher than the thermal front velocity.

In a coordinate system fixed to the surface separating the condensed and gaseous phases the thermal conductivity equation has the form [3]:

$$\frac{\partial T}{\partial t} - v_{sub}\frac{\partial T}{\partial x} = \frac{\partial}{\partial x}\left(a\frac{\partial T}{\partial x}\right), \tag{1}$$

where $v_{sub}$ is the evaporation rate, which depends on the surface temperature $T_s$ and is given by Frenkel's expression [4]:

$$v_{sub} = v_0 \exp\left(-T_{sub}/T_s\right). \tag{2}$$

Physics Institute, Academy of Sciences of the Belorussian SSR. A. V. Sevchenko Scientific-Research Institute for Applied Physics Problems. V. I. Lenin State University, Minsk. Translated from Inzhenerno-Fizicheskii Zhurnal, Vol. 52, No. 5, pp. 817-822, May, 1987. Original article submitted February 26, 1986.

0022-0841/87/5205-0599$12.50  